

# Constraints on Early Star Formation from the 21-cm Global Signal

Piero Madau

*Department of Astronomy & Astrophysics, University of California, 1156 High Street, Santa Cruz, CA 95064, USA*

9 July 2018

## ABSTRACT

The tentative detection by the EDGES experiment of a global 21-cm absorption trough centered at redshift 17 opens up the opportunity to study the birth of the first luminous sources, the intensity of radiation backgrounds at cosmic dawn, the thermal and ionization history of the young intergalactic medium. Here, we focus on the astrophysical implications of the Ly $\alpha$  photon field needed to couple the spin temperature to the kinetic temperature of the gas at these early epochs. Under the basic assumption that the 21-cm signal is activated by extremely metal-poor stellar systems, we show that the EDGES results are consistent with an extrapolation of the declining galaxy UV luminosity density measured at  $4 \lesssim z \lesssim 9$  by deep *HST* observations. A substantially enhanced star formation rate density or new exotic sources of UV photons are not required at the redshifts of the EDGES signal. The amount of ionizing radiation produced by the same stellar systems that induce Ly $\alpha$  coupling is significant, of order 0.5 LyC photons per H-atom per 100 Myr. To keep hydrogen largely neutral and delay the reionization process consistently with recent *Planck* CMB results, mean escape fractions of  $f_{\text{esc}} \lesssim 20\%$  are required at  $z > 15$ .

**Key words:** cosmology: dark ages, reionization, first stars – diffuse radiation – intergalactic medium

## 1 INTRODUCTION

The cosmic microwave background (CMB) spectrum is expected to show an absorption feature at frequencies below 130 MHz imprinted at cosmic dawn, when the universe was flooded with Ly $\alpha$  photons emitted from some of the very first stars and before it was reheated and reionized by Lyman-continuum (LyC) and X-ray radiation (Madau et al. 1997; Tozzi et al. 2000). The absorption signal corresponds to the redshifted 21-cm hyperfine transition of the ground state of neutral hydrogen and arises from the indirect coupling of the spin temperature  $T_S$  to the kinetic temperature  $T_K < T_{\text{CMB}}$  of the intergalactic medium (IGM) via the Wouthuysen-Field effect. The EDGES collaboration has recently reported the detection of a flattened absorption trough – centered at 78 MHz and with an amplitude of 0.5 K – in the sky-averaged radio spectrum that places the onset of this “Ly $\alpha$ -coupling era” at redshift  $z \lesssim 20$ , 180 Myr after the Big Bang (Bowman et al. 2018). The high-frequency cut-off of the EDGES absorption profile suggests that hydrogen was heated to above the CMB temperature less than 100 million years later, at  $z \simeq 15$ . While its anomalous amplitude may indicate the need for new physics or exotic astrophysics (e.g., Barkana 2018; Ewall-Wice et al. 2018; Feng & Holder 2018; Slatyer & Wu 2018), we do not attempt here to ex-

plain this signal altogether. Rather, we focus on the constraints imposed by the required Wouthuysen-Field coupling strength on UV radiation backgrounds and the galaxy emissivity at first light. Such constraints hold under the assumption that the 21-cm signal is activated by young, metal-poor stellar systems regardless of the mechanisms that produce the stronger-than-expected EDGES measurement.

## 2 21-CM RADIATION FROM COSMIC DAWN

We start by briefly reviewing the basic theory of the sky-averaged 21-cm signal from the earliest stages of the galaxy formation process (e.g., Madau et al. 1997; Shaver et al. 1999; Ciardi & Madau 2003; Chen & Miralda-Escudé 2004; Barkana & Loeb 2005; Furlanetto 2006; Pritchard & Loeb 2008; Fialkov et al. 2014; Cohen et al. 2017)). The radiative transfer equation in the Rayleigh-Jeans limit yields the observed brightness temperature relative to the CMB  $T_{21} \equiv (T_S - T_{\text{CMB}})(1 - e^{-\tau})/(1 + z)$ ,

$$T_{21}(\nu_0) \simeq \frac{3c^3 \hbar A_{10} n_{\text{HI}}}{16k_B \nu_{10}^2 H(z)(1+z)} \left(1 - \frac{T_{\text{CMB}}}{T_S}\right), \quad (1)$$

at the frequency  $\nu_0 = \nu_{10}/(1+z)$ . Here,  $\nu_{10} = 1420.4$  MHz is the hyperfine transition frequency of atomic hydrogen,  $T_S$  is

arXiv:1807.01316v2 [astro-ph.CO] 6 Jul 2018

the spin or excitation temperature,  $T_{\text{CMB}} = 2.725(1+z)$  K is the temperature of the CMB,  $A_{10} = 2.87 \times 10^{-15} \text{ s}^{-1}$  is the spontaneous coefficient for the transition,  $n_{\text{HI}}$  is the proper neutral hydrogen density, and  $H(z)$  is the Hubble parameter,  $H(z) \simeq H_0 \sqrt{\Omega_m} (1+z)^{3/2}$  at the redshifts of interest here. Plugging in numbers from the [Planck Collaboration et al. \(2016a\)](#) base  $\Lambda$ CDM cosmology ( $\Omega_m h^2 = 0.1417$ ,  $\Omega_b h^2 = 0.0223$ ,  $h = 0.6774$ ,  $Y_p = 0.245$ ) gives

$$T_{21}(\nu_0) \simeq 26.9 \text{ mK} \left( \frac{1+z}{10} \right)^{1/2} x_{\text{HI}} \left( 1 - \frac{T_{\text{CMB}}}{T_S} \right), \quad (2)$$

where  $x_{\text{HI}}$  is the globally-averaged neutral fraction. The signal will appear in absorption if  $T_S < T_{\text{CMB}}$  and emission otherwise. At the mean gas densities and low temperatures corresponding to the absorption feature reported by the EDGES collaboration, spin-exchange collisions are ineffective, and only the resonant scattering of ambient Ly $\alpha$  radiation can mix the hyperfine levels of the ground state and unlock the spin temperature from the CMB. Assuming steady-state, the fractional deviation of the spin temperature from the temperature of the CMB is given by ([Field 1958](#))

$$1 - \frac{T_{\text{CMB}}}{T_S} = \frac{x_\alpha}{1+x_\alpha} \left( 1 - \frac{T_{\text{CMB}}}{T_K} \right), \quad (3)$$

where  $x_\alpha$  is the Ly $\alpha$  coupling coefficients. Neutral hydrogen is therefore visible against the CMB only if the gas kinetic temperature differs from the CMB temperature and  $x_\alpha > 1$ .<sup>1</sup>

### 3 Ly $\alpha$ COUPLING

The Wouthuysen-Field mechanism ([Wouthuysen 1952](#); [Field 1958](#)) mixes the hyperfine levels of neutral hydrogen via the intermediate step of transitions to the  $2p$  state and is key to the detectability of a 21-cm signal from the epoch of first light. In the cosmological context, we are principally interested in ‘‘continuum’’ photons emitted by the first UV sources between the Ly $\alpha$  and Ly $\beta$  frequencies and redshifted into the Ly $\alpha$  resonance at  $\nu_\alpha = 2.47 \times 10^{15}$  Hz. The coupling coefficient can be written as

$$x_\alpha = \frac{4\pi e^2 f_\alpha T_*}{27 A_{10} T_{\text{CMB}} m_e} S_\alpha n_\alpha, \quad (4)$$

where the factor  $4/27$  relates the  $1 \rightarrow 0$  de-excitation rate via Ly $\alpha$  mixing to the total Ly $\alpha$  scattering rate ([Field 1958](#)),  $T_* \equiv h_P \nu_{10} / k_B = 68.2$  mK,  $f_\alpha = 0.4162$  is the oscillator strength of the Ly $\alpha$  transition, and  $n_\alpha$  is the specific photon number density per unit proper volume at the Ly $\alpha$  frequency

<sup>1</sup> In principle, values of  $x_\alpha < 1$  may be sufficient to achieve a detectable absorption signal if the ratio between the radiation temperature and the gas temperature in Eq. (3) is very large. In order to produce the best-fitting brightness temperature  $T_{21} = -500$  mK observed at the center of the EDGES absorption trough with a coupling coefficient  $x_\alpha < 1$ , this ratio would have to be larger than 27, compared to the value  $T_{\text{CMB}}/T_K = 7$  expected in a standard gas and radiation temperature history. We shall not consider this extreme possibility further in this paper.

in the absence of scattering (in units of  $\text{cm}^{-3} \text{ Hz}^{-1}$ ). The correction factor  $S_\alpha \equiv \int d\nu n_\nu \phi_\nu / n_\alpha$ , where  $\phi_\nu$  is the line profile, accounts for spectral distortions near the resonance ([Chen & Miralda-Escudé 2004](#)). The condition  $x_\alpha = 1$  is satisfied when

$$n_\alpha = n_\alpha^c \equiv 4.2 \times 10^{-20} \text{ cm}^{-3} \text{ Hz}^{-1} \left( \frac{1+z}{18} \right) S_\alpha^{-1}. \quad (5)$$

This ‘‘thermalization’’ photon density corresponds to

$$(n_\alpha^c \nu_\alpha / n_{\text{H}}) \simeq 0.1 [18/(1+z)]^2 S_\alpha^{-1} \quad (6)$$

Ly $\alpha$  photons per hydrogen atom per unit logarithmic frequency interval. Once this value is exceeded, the Wouthuysen-Field effect turns on and drives  $T_S \rightarrow T_K$ . The strength of the Wouthuysen-Field coupling is weakened at low temperatures by atomic recoil, which leads to a distinct dip in the frequency distribution of photons near line center and pushes  $S_\alpha$  below unity (e.g., [Chen & Miralda-Escudé 2004](#); [Hirata 2006](#)). To a good approximation the suppression of the scattering rate can be written as ([Chuzhoy & Shapiro 2006](#))

$$S_\alpha = \exp(-0.013 \tau_{\text{GP}}^{1/3} / T_K^{2/3}), \quad (7)$$

where  $\tau_{\text{GP}} \equiv \pi e^2 f_\alpha n_{\text{HI}} / (m_e H \nu_\alpha)$  is the Gunn-Peterson optical depth and  $T_K$  is in Kelvin. At redshift 17  $\tau_{\text{GP}} = 1.59 \times 10^6$  and the gas temperature is expected to be about 6.9 K in the absence of astrophysical heating or non-standard cooling, so  $S_\alpha \simeq 0.66$ .<sup>2</sup>

In the neutral IGM prior to reionization, photons originally emitted between the Ly $\alpha$  and Ly $\beta$  frequencies will redshift directly into the Ly $\alpha$  resonance, while those emitted at frequencies between Ly $\gamma$  and the Lyman edge will redshift until they reach a Lyman-series resonance and excite a hydrogen atom into the  $np$  configuration ( $n \geq 4$ ). Because the gas is optically thick to Ly $n$  transitions, the excited atom will decay back to  $1s$  in a radiative cascade that ultimately terminates either in a Ly $\alpha$  photon or in two  $2s \rightarrow 1s$  photons. Quantum selection rules and Einstein  $A$  coefficients determine the probability  $P_{np}$  for an H I atom in the  $np$  configuration to generate a Ly $\alpha$  photon,  $P_{np} = (1.000, 0.000, 0.261, 0.308, 0.326, \dots)$  for  $n = (2, 3, 4, 5, 6, \dots)$  ([Hirata 2006](#); [Pritchard & Furlanetto 2006](#)).

Let us now denote with  $\dot{n}_{\nu'}(z')$  the average number of photons emitted per unit comoving volume per unit proper time per unit frequency at redshift  $z'$  and frequency  $\nu'$  by the first generation of UV sources. The resulting photon proper number density at redshift  $z$  and frequency  $\nu_\alpha$  can then be approximated in the limit of large optical depths as a weighted sum over the Ly $n$  levels ([Barkana & Loeb 2005](#); [Hirata 2006](#); [Pritchard & Furlanetto 2006](#); [Meiksin 2010](#))

$$n_\alpha(z) = (1+z)^2 \sum_{n=2}^{\infty} P_{np} \int_z^{z_{\text{max}}(n)} dz' \frac{\dot{n}_{\nu'}(z')}{H(z')}, \quad (8)$$

<sup>2</sup> The above discussion has neglected a second correction to the Wouthuysen-Field coupling, whereby spin-exchange scatterings cause the photon spectrum to relax not to  $T_K$  but to a temperature between  $T_K$  and  $T_S$  ([Chuzhoy & Shapiro 2006](#); [Hirata 2006](#)). This is a small effect, leading to a  $\lesssim 10\%$  reduction in the coefficient  $x_\alpha$  for  $T_K \gtrsim 4$  K.

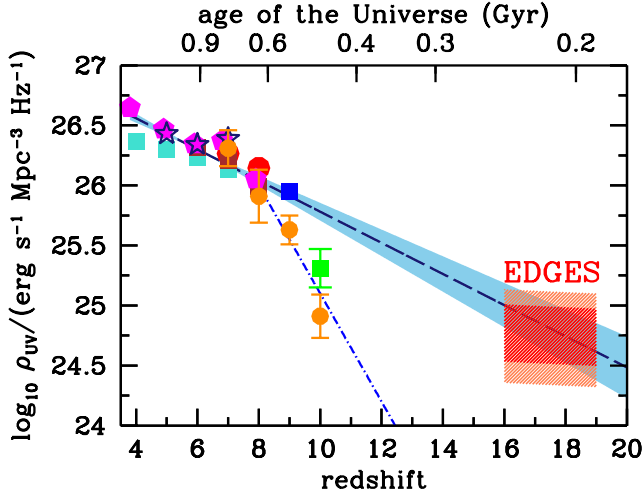


**Figure 1.** Constraints on the epoch of first light with the Wouthuysen-Field effect. The UV luminosity density inferred from the EDGES signal in the “minimal coupling” regime ( $1 \leq x_\alpha \leq 3$ ) is plotted as the shaded red box at  $16 < z < 19$ , for an assumed  $g$  factor of 0.06. The light shading reflects the estimated uncertainty in the  $g$  parameter,  $g = 0.06 \pm 0.02$  (see text for details). The data points show the UV luminosity densities from galaxies using data from Bouwens et al. (2015a) (magenta pentagons), Bowler et al. (2015) (blue stars), Finkelstein et al. (2015) (turquoise squares), Ishigaki et al. (2018) (orange circles), Livermore et al. (2017) (brown squares), McLeod et al. (2015) (blue square), McLure et al. (2013) (red circles), and Oesch et al. (2018) (green square). When computing luminosity densities, all luminosity functions have been integrated down to  $M_{\text{lim}} = -13$ . The dashed line and pale blue shading depict our best-fitting slope for the growth of the galaxy UV luminosity density,  $d \log_{10} \rho_{\text{UV}}/dz = -0.130 \pm 0.018$  (68% confidence interval) in the redshift interval  $4 \leq z \leq 9$ . The dot-dashed curve with  $d \log_{10} \rho_{\text{UV}}/dz = -0.45$  marks the accelerated evolution model of Oesch et al. (2018), a more rapid decline in the galaxy luminosity density at  $z \gtrsim 10$  that is inconsistent with the EDGES signal.

where in each term  $\nu' = \nu_n(1+z')/(1+z)$  is the emitted photon frequency at  $z'$  corresponding to  $1s \rightarrow np$  absorption at  $z$ ,  $\nu_n = (4/3)\nu_\alpha(1-1/n^2)$  is the frequency of the Ly $n$  transition,  $1+z_{\text{max}}(n) = (1+z)\nu_{n+1}/\nu_n$  is the maximum redshift from which a photon entering the Ly $n$  resonance at  $z$  can be observed. Raman scattering in the Lyman series imposes a series of closely-spaced horizons, with the integral in each term of the sum in Equation (8) being carried over redshift intervals,  $\Delta z_n/(1+z) \equiv [z_{\text{max}}(n)-z]/(1+z)$  which become increasingly smaller with higher levels. Higher order cascades contribute then only a small fraction of the total Ly $\alpha$  flux. For photons originally emitted between the Ly $\alpha$  and Ly $\beta$  frequencies, one has  $\Delta z_2/(1+z) = 5/27$ .

#### 4 EARLY STAR-FORMATION

Young, dust-free stellar populations with extremely low metallicities are characterized by very blue rest-frame UV continua, with spectral slopes around  $1500 \text{ \AA}$ ,  $\beta \equiv d \ln f_\lambda/d \ln \lambda$ , approaching the value  $\beta \approx -3$  (Raiter et al. 2010; Schaerer 2003). In this limit the source term  $\dot{n}_\nu$  does not depend on frequency,  $\dot{n}_\nu \propto \nu^{-3-\beta} = \nu^0$ . To account for redshift evolution effects over  $\Delta z_n$ , we write  $\dot{n}_{\nu'}(z') = \dot{n}_{\text{UV}}(z)E(z';z)$ , where we have denoted the ratio of the co-moving photon emissivity at redshift  $z$  to that at redshift  $z' > z$  as  $E(z';z)$  [ $E(z';z) = 1$  in the case of no evolution]. In order to extract the main redshift dependence of the Ly $\alpha$  photon flux in Equation (8), it is convenient to define the following weighted integral

$$\bar{E}_n(z) \equiv \frac{\int_z^{z_{\text{max}}(n)} dz' E(z';z)/H(z')}{\int_z^{z_{\text{max}}(n)} dz'/H(z')} \quad (9)$$

The specific number of photons per unit proper volume at redshift  $z$  and frequency  $\nu_\alpha$  can then be written as

$$n_\alpha(z) = \frac{2(1+z)^{3/2}}{H_0 \sqrt{\Omega_m}} \dot{n}_{\text{UV}}(z)g \quad (10)$$

where

$$g \equiv \sum_{n=2}^{\infty} P_{np} \bar{E}_n(z) \left(1 - \sqrt{\nu_n/\nu_{n+1}}\right). \quad (11)$$

We have folded a variety of parametrization for the redshift evolution law  $E(z';z)$  into the  $g$  term assuming a smoothly-varying monotonic function, and find typical values in the range  $g \simeq 0.04 - 0.09$ , with a contribution to the total Ly $\alpha$  photon flux from  $4 \leq n \leq 20$  Ly $n$  cascades that is typically  $\lesssim 15\%$ . In the case of a non-evolving emissivity and only counting photons originally emitted between the Ly $\alpha$  and Ly $\beta$  frequencies, one has  $g = 0.0814$ .

Substituting now for  $n_\alpha$  in Equation (10) the thermalization photon density  $n_\alpha^c$  (Eq. 5) needed for efficient coupling gives the following constraint on the photon emissivity  $\dot{n}_{\text{UV}}$ ,

$$\dot{n}_{\text{UV}}(z) > \frac{H_0 \sqrt{\Omega_m}}{(1+z)^{3/2}g} \frac{27 A_{10} T_{\text{CMB}} m_e}{8 \pi e^2 f_\alpha T_* S_\alpha}. \quad (12)$$

Plugging in numbers and converting the photon emissivity  $\dot{n}_{\text{UV}}$  into a  $1500 \text{ \AA}$  luminosity density for comparison with lower redshift data,  $\rho_{\text{UV}} = \dot{n}_{\text{UV}}(h_P \nu_{1500})$  (where  $\nu_{1500} = 10^{15.3} \text{ Hz}$ ), we finally derive

$$\rho_{\text{UV}}(z) > 10^{24.52} g_{0.06}^{-1} \left(\frac{18}{1+z}\right)^{1/2} \text{ erg s}^{-1} \text{ Mpc}^{-3} \text{ Hz}^{-1}, \quad (13)$$

where  $g_{0.06} \equiv g/0.06$ . The numerical value on the rhs corresponds to the coupling condition  $x_\alpha = 1$ . The best-case scenario for producing a strong 21-cm absorption signal is to assume  $T_K \ll T_{\text{CMB}}$  and  $x_\alpha \gtrsim 1$ , and in the limit  $T_K \ll T_{\text{CMB}}$  Equation (3) gives  $T_S/T_K = (1+x_\alpha)/x_\alpha$ . Let us then define the regime  $1 < x_\alpha < 3$  as one of “minimal coupling”, where the spin temperature approaches the

gas temperature from above to within  $1.33 < T_S/T_K \leq 2$ . This minimal coupling regime corresponds to a UV luminosity density in the range  $\rho_{UV} = 10^{24.52} - 10^{25.0} g_{0.06}^{-1} [18/(1+z)]^{1/2} \text{ erg s}^{-1} \text{ Mpc}^{-3} \text{ Hz}^{-1}$ .

In Figure 1 we have plotted this range as a shaded red box in the interval  $16 < z < 19$ , the approximate duration of the EDGES 21-cm absorption trough when efficient coupling must be maintained. The figure also shows the UV luminosity density at  $5 \lesssim z \lesssim 10$  obtained by integrating the observed galaxy luminosity function down to a threshold  $M_{\text{lim}} = -13$ . A turn-over in the  $z \sim 7$  luminosity function at these faint magnitudes is inferred by combining the abundance matching technique with detailed studies of the color-magnitude diagram of low-luminosity dwarfs in the Local Group (Boylan-Kolchin et al. 2015). Interestingly, the Ly $\alpha$  background flux inferred from the EDGES signal is entirely consistent with an extrapolation of UV measurements at lower redshifts, and does not require a substantially enhanced star formation or new exotic sources. The function  $\log_{10}(\rho_{UV}/\text{erg s}^{-1} \text{ Mpc}^{-3} \text{ Hz}^{-1}) = (26.30 \pm 0.12) + (-0.130 \pm 0.018)(z - 6)$ , depicted by the blue shading, is the our best fit for the growth of the galaxy UV luminosity density down to  $M_{\text{lim}} = -13$  mag and over the redshift interval  $4 \leq z \leq 9$ . If our analysis is correct, it would appear that galaxy luminous mass built up at a remarkably steady rate over the first Gyr of cosmic history. Intriguingly, the same scaling also predicts inefficient Wouthuysen-Field coupling and therefore no signal at  $z > 20$ , in agreement with the EDGES observations. As noted by (Kaurov et al. 2018), however, the sharpness of the brightness temperature drop between  $z = 21$  and 19 suggests that the spin temperature of neutral hydrogen was coupled to the kinetic temperature of the gas very rapidly, within a small fraction of a Hubble time. This requires the Ly $\alpha$  background to decline at  $z > 20$  more abruptly than expected from the  $d \log_{10} \rho_{UV}/dz = -0.130$  evolution.

Figure 1 also displays (dot-dashed curve with  $d \log_{10} \rho_{UV}/dz = -0.45$ ) the accelerated evolution suggested by the dearth of galaxies brighter than  $-17$  mag at  $z \sim 10$  in *Hubble Space Telescope* (*HST*) deep fields (Oesch et al. 2018; Ishigaki et al. 2018). Based on a comprehensive search in all prime *HST* datasets, Oesch et al. (2018) have recently shown that the UV luminosity function decreases by one order of magnitude from  $z \sim 8$  to  $z \sim 10$  over a four magnitude range, a drop that may signal a shift of star formation toward less massive, fainter galaxies. The lower normalization – if not accompanied by a steepening of the faint-end slope with redshift – implies a rapid decrease of the total UV luminosity density at these epochs, a decline that extrapolated to  $z \gtrsim 15$  is clearly inconsistent with the EDGES signal. The debate about the UV luminosity function at  $z \sim 10$  is far from settled, however, and the *HST* and EDGES observations may hint at a possible differential evolution of bright vs. faint galaxies (Mason et al. 2015; Mirocha & Furlanetto 2018).

## 5 IONIZING PHOTON PRODUCTION

Strictly speaking, of course, the 21-cm coupling constraints plotted in Figure 1 should be considered only as a lower limit to the UV luminosity density at  $16 < z < 19$ . It is instruc-

tive, at this stage, to estimate the emission above the Lyman limit expected by the same galaxies that induce strong Ly $\alpha$  coupling. Population synthesis models predict an ionizing photon production efficiency per unit stellar mass that increases with decreasing metallicity and for initial mass functions (IMFs) favouring the formation of very massive stars (Schaerer 2003). Here, we are interested in the LyC output per unit UV luminosity density,  $\xi_{\text{ion}} \equiv \int_{\nu_L} d\nu \dot{n}_\nu / \rho_{UV}$ , where  $\nu_L$  is the hydrogen Lyman edge. For extremely metal-poor as well as young (zero age main sequence) stellar populations, the ionizing photon yield is only weakly dependent on the IMF and converges to the narrow range of values  $\log_{10}(\xi_{\text{ion}}/\text{erg}^{-1} \text{ Hz}) = 26 - 26.2$  (Raiter et al. 2010). Constant star-formation rate models reach an equilibrium value of the yield  $\xi_{\text{ion}}$  that is 0.1-0.15 dex smaller in the case of massive IMFs, and even smaller for “normal” IMFs. These yields are consistent with those estimated from H $\alpha$  emission line fluxes in the bluest and faintest galaxies at  $5.1 < z < 5.4$ ,  $\log_{10}(\xi_{\text{ion}}/\text{erg}^{-1} \text{ Hz}) = 25.9_{-0.2}^{+0.4}$  (Bouwens et al. 2016).

Extremely metal-poor stellar systems with a UV luminosity density of  $\rho_{UV} = 10^{24.82} g_{0.06}^{-1} [18/(1+z)]^{1/2} \text{ erg s}^{-1} \text{ Mpc}^{-3} \text{ Hz}^{-1}$ , corresponding to a coupling coefficient  $x_\alpha = 2$ , will then produce somewhere in the range of

$$\frac{\xi_{\text{ion}} \rho_{UV}}{n_{\text{H}}} \simeq 0.3 - 0.6 g_{0.06}^{-1} \left( \frac{18}{1+z} \right)^{1/2} \left( \frac{x_\alpha}{2} \right) \quad (14)$$

ionizing photons per H-atom per 100 Myr, where the scaling with coupling strength has been made explicit for clarity. Of these, only a globally-averaged fraction  $f_{\text{esc}}$  will escape from individual galaxies, make it into the IGM, and initiate the process of reionization by creating expanding H II bubbles in the neutral cosmic gas. Since photoionizations dominate over radiative recombinations at these redshifts, the “reionization equation” for the time evolution of the volume-averaged hydrogen ionized fraction,

$$\frac{dx_{\text{HII}}}{dt} = f_{\text{esc}} \frac{\xi_{\text{ion}} \rho_{UV}}{n_{\text{H}}}, \quad (15)$$

can be easily integrated. The escape fraction is constrained by the latest *Planck* CMB anisotropy and polarization data analysis, which yields a small Thomson scattering optical depth of  $\tau_{\text{es}} \simeq 0.055 - 0.060$ , with  $\sigma(\tau_{\text{es}}) \sim 0.01$  (Planck Collaboration et al. 2016b); a redshift-asymmetric parameterization of the ionized fraction gives  $z_{\text{beg}} = 10.4_{-1.6}^{+1.9}$  for the redshift (“beginning” of reionization) where  $x_{\text{HII}} = 10\%$ , and leaves little room for any significant ionization at  $z > 15$ . More specifically, a recent non-parametric reconstruction of the history of reionization applied to *Planck* intermediate 2016 data finds a 68% upper limit to the electron fraction at  $z = 15$  of 8% (flat  $\tau_{\text{es}}$  prior, see Millea & Bouchet 2018).

A fiducial model with  $\xi_{\text{ion}} \rho_{UV}/n_{\text{H}} = 0.5 [18/(1+z)]^{1/2}$  ionizing photons per H-atom per 100 Myr would require then, according to Equation (15), mean escape fractions  $f_{\text{esc}} \lesssim 20\%$  to keep the early IGM largely neutral and delay the reionization process consistently with *Planck* results. Any early stellar systems producing a larger Ly $\alpha$  background intensity would emit more LyC and X-ray radiation, generating more ionizations and gas heating which would tend to make the depth and duration of the absorption signal

smaller. For comparison, studies of the reionization history at later epochs have shown that, when assuming a limiting magnitude of  $M_{\text{lim}} = -13$  and  $\log_{10}(\xi_{\text{ion}}/\text{erg}^{-1}\text{Hz}) = 25.2\text{--}25.5$ , average escape fractions from galaxies of 10–20% produce the requisite number of LyC radiation to complete reionization by  $z = 6$  (e.g., Bouwens et al. 2015b; Finkelstein et al. 2015; Robertson et al. 2015; Madau 2017) with no contribution from other sources.

## 6 SUMMARY

The 21-cm global signal is a window into the earliest star formation in the universe. In this study we have ignored the anomalous depth of the EDGES absorption feature, and concentrated instead on the implications for early star formation of the Ly $\alpha$  photon field required to couple the spin temperature of the hyperfine levels to the gas temperature. Under the basic assumption that the 21-cm signal is activated by young, metal-poor stellar systems, we have shown that the EDGES signal is consistent with an extrapolation of the evolving galaxy UV luminosity density measured at  $4 \lesssim z \lesssim 9$  by deep *HST* observations. Models of accelerated evolution where the UV luminosity density declines rapidly at  $z \gtrsim 10$  are unable to provide the needed Ly $\alpha$  coupling strength at  $z \lesssim 20$ . If our analysis is correct and the EDGES results are confirmed, galaxy light appears to have built up at a surprisingly steady rate over the first Gyr of cosmic history; in other words, a substantially enhanced star formation rate density or exotic luminous sources do not seem to characterize the epoch of first light. The amount of ionizing radiation expected by the same systems that induce strong Ly $\alpha$  coupling is significant, of order 0.3–0.6 LyC photons per H-atom per 100 Myr at these epochs. To keep the early IGM largely neutral and delay the reionization process consistently with *Planck* CMB results, our estimates imply mean escape fractions into the IGM  $f_{\text{esc}} \lesssim 20\%$ .

Since we have focused on the evolution of the cosmic UV emissivity, the constraints discussed here – while still uncertain – are rather model independent, as we have tried to keep assumptions regarding the nature of the first luminous sources to a minimum. The present analysis should be regarded as complementary to those of, e.g., Mirocha & Furlanetto (2018) and Kaurov et al. (2018), who have recently explored the consequences of the EDGES results on the star formation efficiencies of dark matter halos at early times. We finally note that, in the presence of some other 21-cm background of specific intensity  $J_{21}$ , the brightness temperature of such radio emission should be added to  $T_{\text{CMB}}$  in all the above equations,  $T_{\text{CMB}} \rightarrow T_R = T_{\text{CMB}} + c^2 J_{21} / (2k_B \nu_{10}^2)$ . A radio background excess (Ewall-Wice et al. 2018; Feng & Holder 2018) would require an even larger Ly $\alpha$  radiation field in order to achieve efficient coupling.

## ACKNOWLEDGMENTS

The author would like to thank R. Bouwens and A. Meiksin for many useful discussions on the topics presented here. Support for this work was provided by NASA through a

contract to the WFIRST-EXPO Science Investigation Team (15-WFIRST15-0004), administered by the GSFC.

## REFERENCES

- Barkana R., 2018, *Nature*, **555**, 71  
 Barkana R., Loeb A., 2005, *ApJ*, **626**, 1  
 Bouwens R. J., et al., 2015a, *ApJ*, **803**, 34  
 Bouwens R. J., Illingworth G. D., Oesch P. A., Caruana J., Holwerda B., Smit R., Wilkins S., 2015b, *ApJ*, **811**, 140  
 Bouwens R. J., Smit R., Labbé I., Franx M., Caruana J., Oesch P., Stefanon M., Rasappu N., 2016, *ApJ*, **831**, 176  
 Bowler R. A. A., et al., 2015, *MNRAS*, **452**, 1817  
 Bowman J. D., Rogers A. E. E., Monsalve R. A., Mozdzen T. J., Mahesh N., 2018, *Nature*, **555**, 67  
 Boylan-Kolchin M., Weisz D. R., Johnson B. D., Bullock J. S., Conroy C., Fitts A., 2015, *MNRAS*, **453**, 1503  
 Chen X., Miralda-Escudé J., 2004, *ApJ*, **602**, 1  
 Chuzhoy L., Shapiro P. R., 2006, *ApJ*, **651**, 1  
 Ciardi B., Madau P., 2003, *ApJ*, **596**, 1  
 Cohen A., Fialkov A., Barkana R., Lotem M., 2017, *MNRAS*, **472**, 1915  
 Ewall-Wice A., Chang T.-C., Lazio J., Doré O., Seiffert M., Monsalve R. A., 2018, preprint, ([arXiv:1803.01815](https://arxiv.org/abs/1803.01815))  
 Feng C., Holder G., 2018, *ApJ*, **858**, L17  
 Fialkov A., Barkana R., Visbal E., 2014, *Nature*, **506**, 197  
 Field G. B., 1958, *Proceedings of the IRE*, **46**, 240  
 Finkelstein S. L., et al., 2015, *ApJ*, **810**, 71  
 Furlanetto S. R., 2006, *MNRAS*, **371**, 867  
 Hirata C. M., 2006, *MNRAS*, **367**, 259  
 Ishigaki M., Kawamata R., Ouchi M., Oguri M., Shimasaku K., Ono Y., 2018, *ApJ*, **854**, 73  
 Kaurov A. A., Venumadhav T., Dai L., Zaldarriaga M., 2018, preprint, ([arXiv:1805.03254](https://arxiv.org/abs/1805.03254))  
 Livermore R. C., Finkelstein S. L., Lotz J. M., 2017, *ApJ*, **835**, 113  
 Madau P., 2017, *ApJ*, **851**, 50  
 Madau P., Meiksin A., Rees M. J., 1997, *ApJ*, **475**, 429  
 Mason C. A., Trenti M., Treu T., 2015, *ApJ*, **813**, 21  
 McLeod D. J., McLure R. J., Dunlop J. S., Robertson B. E., Ellis R. S., Targett T. A., 2015, *MNRAS*, **450**, 3032  
 McLure R. J., et al., 2013, *MNRAS*, **432**, 2696  
 Meiksin A., 2010, *MNRAS*, **402**, 1780  
 Millea M., Bouchet F., 2018, preprint, ([arXiv:1804.08476](https://arxiv.org/abs/1804.08476))  
 Mirocha J., Furlanetto S. R., 2018, preprint, ([arXiv:1803.03272](https://arxiv.org/abs/1803.03272))  
 Oesch P. A., Bouwens R. J., Illingworth G. D., Labbé I., Stefanon M., 2018, *ApJ*, **855**, 105  
 Planck Collaboration Ade P. A. R., Aghanim N., Arnaud M., et al. 2016a, *A&A*, **594**, A13  
 Planck Collaboration Adam R., Aghanim N., Ashdown M., et al. 2016b, *A&A*, **596**, A108  
 Pritchard J. R., Furlanetto S. R., 2006, *MNRAS*, **367**, 1057  
 Pritchard J. R., Loeb A., 2008, *Phys. Rev. D*, **78**, 103511  
 Raiter A., Schaerer D., Fosbury R. A. E., 2010, *A&A*, **523**, A64  
 Robertson B. E., Ellis R. S., Furlanetto S. R., Dunlop J. S., 2015, *ApJ*, **802**, L19  
 Schaerer D., 2003, *A&A*, **397**, 527  
 Shaver P. A., Windhorst R. A., Madau P., de Bruyn A. G., 1999, *A&A*, **345**, 380  
 Slatyer T. R., Wu C.-L., 2018, preprint, ([arXiv:1803.09734](https://arxiv.org/abs/1803.09734))  
 Tozzi P., Madau P., Meiksin A., Rees M. J., 2000, *ApJ*, **528**, 597  
 Wouthuysen S. A., 1952, *AJ*, **57**, 31

This paper has been typeset from a  $\text{\TeX}/\text{\LaTeX}$  file prepared by the author.